

Estimation of Shade Losses in Unlabeled PV Data

Bennet Meyers^{1,2} and David Jose Florez Rodriguez²

¹ SLAC National Accelerator Laboratory, Menlo Park, CA, 94025, USA

² Stanford University, Stanford, CA, 94305, USA

Abstract—We provide a methodology for estimating the losses due to shade in power generation data sets produced by real-world photovoltaic (PV) systems. We focus this work on estimating shade loss from data that are unlabeled, *i.e.* power measurements with time stamps but no other information such as site configuration or meteorological data. This approach enables, for the first time, the analysis of data generated by small scale, distributed PV systems, which do not have the data quality or richness of large, utility-scale PV systems or research-grade installations. This work is an application of the newly published signal decomposition (SD) framework, which provides an extensible approach for estimating hidden components in time-series data.

Index Terms—photovoltaic systems, solar energy, distributed power generation, energy informatics, signal processing, machine learning, statistical learning, unsupervised learning

I. INTRODUCTION

The distributed rooftop solar market is growing rapidly, with 3.2 GW_{DC} of residential PV installed in the U.S. in 2020, the largest year on record [1]. While utility solar continues to contribute the majority of new installations, 46% of new installed capacity in 2020 (5.3 GW_{dc}) were non-utility, distributed systems [1]. Clearly, distributed PV systems continue to account for a significant fraction of solar power generation.

However, distributed PV presents a distinct challenge for data analysis, as compared to utility PV plants. We call the data that come from utility power plants *labeled*. Generally speaking, this means the power production data comes with supplementary data and information such as correlated measurements from meteorological stations and system configuration information from engineering drawings. In contrast, distributed PV tends to generate *unlabeled* and *partially labeled* data sets, making it difficult or impossible to calculate a performance index for the systems (see [2] for definition and description of performance index in this context).

In this manuscript, we present and validate a novel approach for estimating the shade losses in PV systems from unlabeled production data, *i.e.*, the measured power output of the system over a multi-year period. We assume that the power measurements are taken on regular intervals on a sub-daily basis, typically in the range of every 5 minutes to once an hour. The method takes the unlabeled data for a single PV system as an input, and returns an estimate of the energy lost to shade. Our approach is an application of the *signal decomposition (SD)*

framework [3], in which we model the shade loss as one of a number of component processes which combine to generate the observed signal. The methods proposed in this paper are available as a module in the Solar Data Tools package [4], [5].

II. BACKGROUND AND RELATED WORK

The non-linear loss of power generation in PV systems experiencing partial shade has long been known to be a major concern in real world systems, particularly for distributed PV in urban environments [6]–[8]. Generally speaking, prior research into quantifying shade losses in operational PV systems has focused on generating a high quality model of the system in question to use as a reference [9]–[11] or utilizing additional data sources, such as an unshaded reference system [12] or current-voltage response measurements (*i.e.*, IV curves) [13].

In this paper, we develop a methodology for estimating the soiling losses in unlabeled PV system power generation data, *i.e.*, a time series of real power measurements and nothing else. This approach, while admittedly less accurate than some of the methods mentioned above, unlocks large swaths of real-world production data that otherwise could not be analyzed for shade loss. Additionally, the analysis is easily automated, enabling the analysis of large fleets of heterogeneous PV systems. This approach is based on a framework of signal decomposition (SD), and a summary of the long history of signal decomposition and many related topics involved is available in [3, §3].

III. METHODS

We construct an SD problem [3] that models the decomposition of the power data into components that represent weather effects, a clear sky base line, and shade losses. This approach can be thought of as an *unsupervised* machine learning (ML) method for finding structure in time series data, similar to model-based clustering methods like Gaussian mixture models [14, §14.3.7]. Unlike supervised ML, there is no “training” of the method; we simply design the mathematical optimization problem, input the data for analysis, and receive the estimate of the shade losses.

As important as the formulation of the SD problem, however, is how the raw power data is prepared for analysis. Before estimating the components, the power data is filtered and transformed in a way that emphasizes the periodic nature of fixed shade patterns, both day-to-day as well as season-to-season and year-to-year. We find that putting the data in a particular form is critical to being able to apply the SD framework to this problem.

This material is based on work supported by the U.S. Department of Energy’s Office of Energy Efficiency and Renewable Energy (EERE) under the Solar Energy Technologies Award Number 38529.

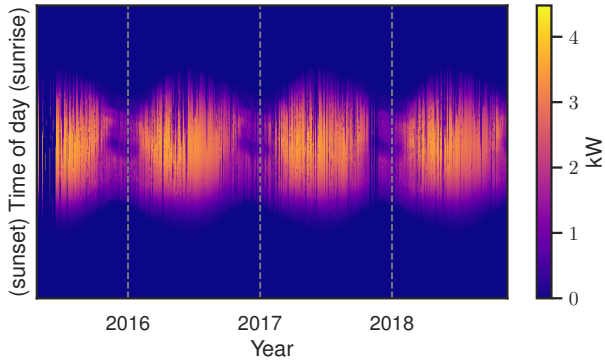


Fig. 1. An example multi-year, unlabeled power data set, with noticeable shade in the winter.

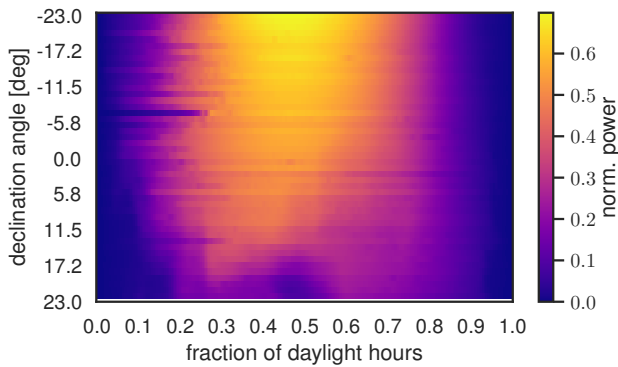


Fig. 2. The output of the data preparation procedure for the data shown in figure 1. We call this the “transformed” data.

In the remainder of this section, we describe the data preparation, SD formulation, and validation procedure.

A. Data preparation

We begin with a multi-year data set of measured power from a PV system, that may or may not have shade. A typical example is shown in figure 1, with the 5-minute real power measurements represented as a heatmap with lighter pixels representing higher power. In this view, days are columns of pixels, starting with sunrise on the top of the image and ending with sunset at the bottom. Consecutive days go left to right. The seasons are visible as a shortening and lengthening of the day, seen as width of the bright portion. This example happens to have noticeable shade in the winter months, observable as a dark patch in the middle of the shorter days. We can already observe that this pattern repeats itself on a yearly basis and has a different character than power lost to clouds, which are seen as dark, vertical lines.

The end result of the data preparation process for this example is shown in figure 2. In the remainder of this section, we will describe how this second figure is generated.

a) Onboarding: First, the data is onboarded and standardized using Solar Data Tools (SDT) [4], [5]. This accounts for gaps in data or missing time stamps and puts the data in

the 2D array form shown in figure 1. Gaps in the original data are either linearly interpolated or zero-filled depending on if it is day or night. The software has tools for correcting common errors in PV data sets such as time shifts due to daylight savings clock changes.

b) SDT data labeling: With the original scalar time series now embedded in a matrix, we use two additional features of SDT: clear day detection and sunrise/sunset detection. The first subroutine automatically segments the data by categorizing days as being (more) sunny or (more) cloudy. The second subroutine analyzes the matrix embedding of the power signal to make a robust estimate of local sunrise and sunset times each day. (These may be calculated exactly using well known equations if the latitude and longitude of the PV systems is known, but we assume *no* access to outside information besides the measured power.) We note briefly here that both these subroutines in SDT make use of the SD framework [3] and operate on the general principle of detecting a structured component within a signal.

c) Soiling estimation and correction: Next, we apply a method for detecting soiling trends in unlabeled PV power data sets, which is described in soon to be published manuscript [15] and also makes use of an SD framework. As described in [15, §3-D], we use the estimated soiling component to correct the measured data, generating a new estimate of system power, with the soiling losses simply removed. This procedure is analogous to generating a performance index that accounts for estimated soiling, but it does not require any additional information besides power to construct. We find that removing detected soiling trends in the data yields a significant improvement in the subsequent shade analysis.

d) Masking and resampling: Using the estimates of sunrise and sunset times, a mask is generated to remove the night time data. This results in a different number of data points each day, as the length of the day changes, so the resulting signals are upsampled using linear interpolation to all have the same number of samples per day, chosen to be 256. (This value is selected somewhat arbitrarily to be a power of 2 larger than any of the resulting day-long signal segments.) Additionally at this step, the data is normalized to be in the range $[0, 1]$. This results in a transformation of the original power matrix shown in figure 3. We observe that the days have been “stretched” so that they all appear to be the same length.

e) Averaging by declination angle bin: The final step is to average the data across seasons and years, excluding the cloudy days detected with SDT. We do this by assigning a *declination angle* to each day, which is the angular position of the sun at solar noon, with respect to the plane of the equator, and is given by a simple equation based only on the day of year [16, §1.6]. We then bin the declination angle values, and keeping only the (more) sunny days, we average the daily signals in each bin. Finally, we arrange the bin in sequential order, producing the tabular data set shown in figure 2. If for whatever reason there are no data available to average for a particular bin (*e.g.*, due to missing data and bad weather,

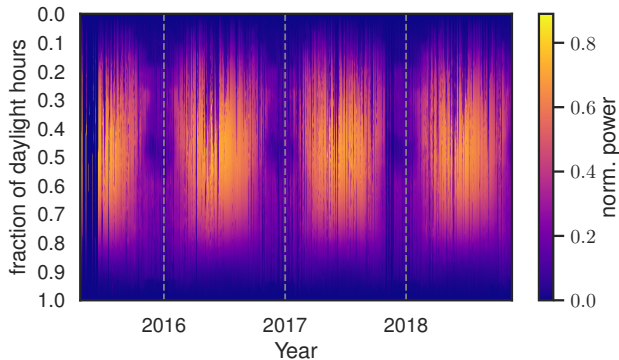


Fig. 3. The result of the masking and resampling step in the data preparation procedure.

no clear sky data was recorded at that declination angle), we simply fill that row with missing values markers, or ‘?’ in the notation of SD [3].

We treat this tabular data representation as the vector-valued input y to the SD problem. Using the notation from [3]), this gives us dimensions for our SD problem of $T = 47$ and $p = 256$.

B. SD problem formulation

Utilizing the notation of signal decomposition defined in [3], we say that our data for this SD problem instance is a signal $y \in (\mathbf{R} \cup \{?\})^{T \times p}$ with length $T = 47$ is the number of declination angle bins and $p = 256$ is the number of upsampled normalized power measurements in one day. In other words, our signal, y , is a matrix of size 47 by 256, possibly with missing values. We model the signal y as the composition of $K = 3$ components, x^1 to x^3 , the sum of which must be equal to the signal y at the entries that do not contain missing values, or in other words,

$$y_{t,i} = x_{t,i}^1 + x_{t,i}^2 + x_{t,i}^3, \text{ for } t \in \mathcal{K},$$

where \mathcal{K} is the set of indices (t, i) that do not contain missing values (*i.e.*, the “known” set). The three components are defined in the SD model by their cost functions $\phi_k(x^k)$ for $k = 1, \dots, 3$. (We drop the superscript k on x to keep the notation lighter when not distinguishing between particular components.) Following the convention in [3], we assign the first component x_1 the role of the “residual” and the last component x_3 to be what we are interested in calculating, in this case shade loss. (We think of this ordering as “building” the SD model, by accounting for sourcing of variation in the data before arriving at the component of interest.) Below, we describe each of these components and their mathematical definition within the SD framework.

a) Component x^1 : The first component represents the residual of the model, and it represents the remaining variability due to weather that was not removed through the clear

day filtering with SDT. It is taken to be the sum-absolute cost function [17, §6.1],

$$\phi_1(x) = \sum_{(t,i)} |x_{t,i}|, \quad (1)$$

which is chosen for its robustness to outliers and preference for values that are exactly zero.

b) Component x^2 : We construct the second component to represent the unobstructed clear sky behavior of a fixed-tilt PV system. We define $\phi_2(x)$ to represent the distance from a corpus of clear sky signals for all possible tilts and azimuth, generated by pvlib-python [18], and then normalized and transformed the same as the measured data. We follow the methodology described in [3, §6.3] for fitting a component class loss to a corpus of signals known to belong to the class. This is done by first calculating the statistical mean μ and covariance Σ of the signal corpus, arranged as a matrix. Then, we generate a low-rank approximation calculating the eigendecomposition [19, §8] of the empirical covariance,

$$\Sigma = Q\Lambda Q^{-1},$$

and keeping the top $k = 6$ eigenvalues, giving us $Q_k \in \mathbf{R}^{p \times k}$ and $\Lambda_k = \text{diag}(\lambda_k)$ with $\lambda_k \in \mathbf{R}^k$. We then construct the component cost as the linear combination of three constituent costs

$$\phi_2(x) = \lambda_{2a} \ell_{2a}(x) + \lambda_{2b}(x) \ell_{2b} + I_2(x), \quad (2)$$

where $\ell_{2a}, \ell_{2b} : \mathbf{R}^{T \times p} \rightarrow \mathbf{R}$ are continuous functions, $\lambda_{2a}, \lambda_{2b}$ are scalar problem weights, and $I_2 : \mathbf{R}^{T \times p} \rightarrow \{0, \infty\}$ is an indicator function of a set of equality and inequality constraints imposed on the second component. The first loss applies regularization to a helper variable which will indicate how much of which corpus eigenvectors to use,

$$\ell_{2a}(x) = \|Mz_2\|_F,$$

with $z_{2a} \in \mathbf{R}^{k \times p}$ is the new variable in the SD optimization problem and $M \in \mathbf{R}^{T \times k}$. The function $\|\cdot\|_F$ is the standard Frobenius matrix norm [17, §A.1.1]. The matrix M is calculated from the reduced eigenvalues calculated earlier,

$$M = \begin{bmatrix} \text{diag}(1/\lambda_k) \\ \mathbf{0} \end{bmatrix}.$$

The second loss selects for components that change smoothly with changing declination angle,

$$\ell_{2b}(x) = \|D_2x\|_F,$$

where $D_2 \in \mathbf{R}^{(T-2) \times T}$ is the second-order discrete difference operator. (See, for example, [20, §6.4] for information on difference matrices.) In other words, these first two terms tell us that we want signals that are similar to our corpus, and changing smoothly day-to-day. Finally, the constraints in I_2 are the union of the following

$$\begin{aligned} \{x \mid x \succeq 0\} \\ \{x \mid D_2x \preceq 0\} \\ \{x \mid x_{t,i} = 0 \text{ for all } t \text{ and } i \in \{1, 256\}\} \\ \{x \mid x - \mu = z_2^T Q_r^T\}. \end{aligned}$$

TABLE I
SD PROBLEM PARAMETERS

param.	value	description
λ_{2a}	0.5	penalizes distance of clear sky component from corpus of reference signals
λ_{2b}	1×10^3	encourages smoothness of clear sky component along declination angle axis
λ_3	1	encourages compact shade component

Briefly, this constrains the component to (1) be non-negative, (2) have non-positive curvature along the the first axis (declination angle), (3) start and end at zero along the second axis (fraction of day), and (4) be a combination of corpus eigenvectors. Taken altogether, we have constructed a component class ϕ_2 that is bespoken for this particular analysis and provides a baseline to reference the losses due to shade in the data.

c) *Shade component*: The third component represents the shade losses in the system. We define it mathematically as

$$\phi_3(x) = \lambda_3 (\|D_2x\|_F + \|D_2x^T\|_F) + I_-(x),$$

where λ_3 is a problem parameter and I_- is the indicator function of the nonpositive orthant. This cost encourages component values that do not fluctuate wildly along either axis (declination angle or day fraction) and are nonpositive (shade can only reduce the power production). A key insight of our data preparation process is that in the transformed data space, periods of shade tend to be “compact”, *i.e.*, well localized in space with clear boundaries.

C. SD parameters

The SD problem formulation includes three parameters, λ_{2a} , λ_{2b} , and λ_3 . These parameters are tunable, and different values can greatly affect the characteristics and quality of the resulting decomposition. A deep discussion on the role of parameters in SD problems can be found in [3, §2.6]. While a method is provided in [3, §2.7] for selecting optimal parameter values, we find that in this context it makes more sense to rely on the practical experience of the analyst. In other words, we have found values that work well in many cases, and a small amount of hand-tuning is accepted in other cases. A description of these parameters and their default values are given in table I.

D. Validation

As described in detail in [21], a small fleet of 25 rooftop PV installations in Southern California has been modeled in pvlib-python [18]. We briefly describe the procedure here but refer readers to that paper for a complete description of the modeling building process.

We estimate the unobstructed power output of the system over a typical clear sky year, making use of the simplified Solis clear sky model [22] available in pvlib-python [18]. This provides us with a reference estimate for the unshaded power production of these systems, which we can use to validate the estimate from the SD formulation.

In this paper, we validate the proposed method for shade loss estimation based on signal decomposition by using the pvlib models of the systems as a reference. An estimate of the shade loss under clear sky conditions is generated for each site by comparing the sunny days from the data set to the pvlib model. This calculation is taken as the ground truth, and we then calculate errors between the SD estimate and the pvlib estimate.

IV. RESULTS

In this section, we present a validation of the proposed SD methodology for shade loss estimation. We compare the estimates of shade loss generated by the SD methodology to the estimates derived from modeling the sites in pvlib-python, as described in [21]. First, we discuss in more detail a case study of a single site. Then we discuss the analysis of the fleet.

We find that the proposed method clearly detects losses in the systems that are consistent with the pvlib estimates of shade loss. For low-to-medium shaded systems that have azimuth orientations within 90° of due south, the method does quite well in capturing the temporal impacts of shade and estimating the total losses. As the shade losses get more extreme, the SD methodology tends to conservatively under-predict the total losses. Conversely, we find that the SD methodology tends to *over*-predict shade losses for systems with azimuths pointing due east and west. Improving the performance of the algorithm systems with these azimuths will be an area of future research.

A. Case study

A typical example data set from the validation fleet of 25 systems is shown in figure 1. The resulting decomposition for this data set is shown in figure 4, with the components displayed in the transformed data space.

We can view the decomposition in the original time series space by undoing the data transformation process. A selection of days and their SD decompositions are shown in figure 5, along with the pvlib estimates of clear sky power output and soiling loss. We see good general agreement, but we note that the SD model is tending to underpredict the clear sky component under highly shaded conditions, as seen in the winter. This is reasonable given our model formulation and lack of any other reference. We generally prefer for the smallest reasonable decomposition that explains the data. (Note that the loss can be made arbitrarily large by increasing the magnitude of the clear sky component.)

An analysis of the shade losses in a typical year for this data set is shown in figure 6. We see, again, that the SD model tends to be conservative; the proposed algorithm estimates a lower clear sky baseline in the winter than the pvlib estimate, resulting in smaller estimated shade losses in the winter. However, the SD estimate of shade losses is of the correct magnitude and has the same seasonal structure as what we estimate using pvlib.

We calculate two summary error metrics from this yearly analysis: (1) the shade loss root-mean-square error (RMSE)

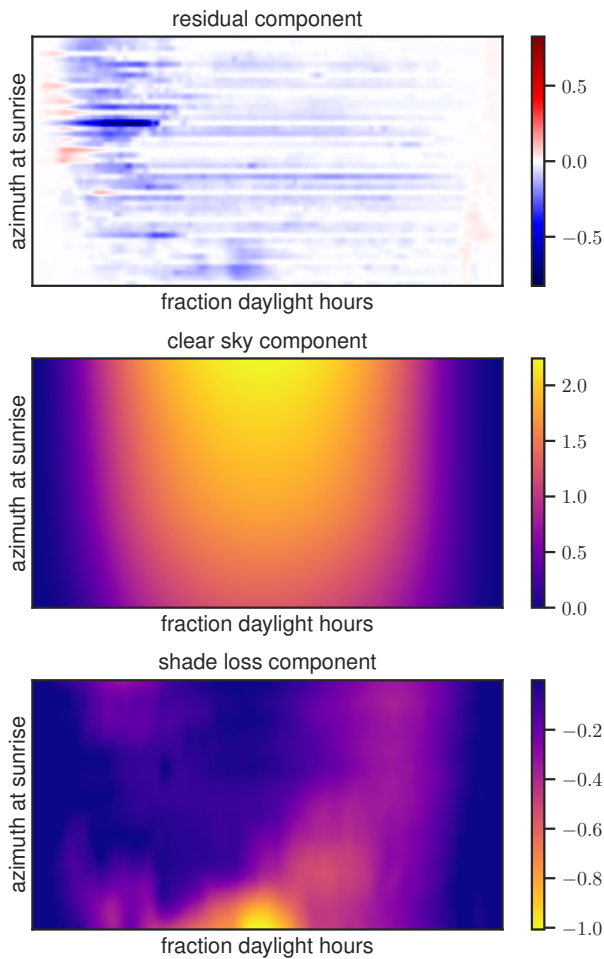


Fig. 4. The calculated decomposition of the signal shown in figure 2. Top, the weather component. Middle, the clear sky component. Bottom, the shade loss component.

and (2) the difference between pv-lib and SD estimates of total yearly shade loss as a percentage of total yearly energy (RE, for “relative error”). For this example, the RMSE is 1.61 kWh and the difference in energy loss is 2.8%.

B. Fleet study

We present the RMSE and RE for the 25 sites in the validation fleet in figures 7 and 8 respectively. We hand labeled each of the 25 sites as one of three bins: low (L), medium (M), and high (H) shade losses. The mean and standard deviation of these metrics are given for each bin in table II We observe that the high-shade bin include sites that are the largest outliers, and that those high error sites are negative, *i.e.*, the SD method under-predicts the amount of shade. Additionally, this effect gets larger with more aggressive shade. An extreme example is shown in figure 9. Visual inspection of this site confirms trees directly to the south of the system, which project shade all day long. As expected, SD estimates a smaller clear sky envelope for the data, evidently the smallest such envelop that is consistent with the data. However, we note that the SD

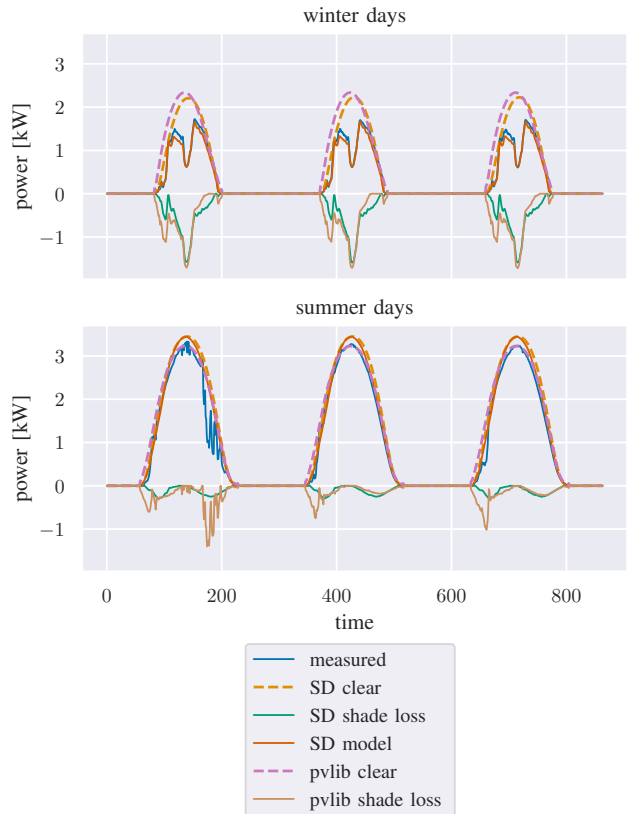


Fig. 5. The calculated decomposition of the signal shown in figure 2, shown as a time series plot.

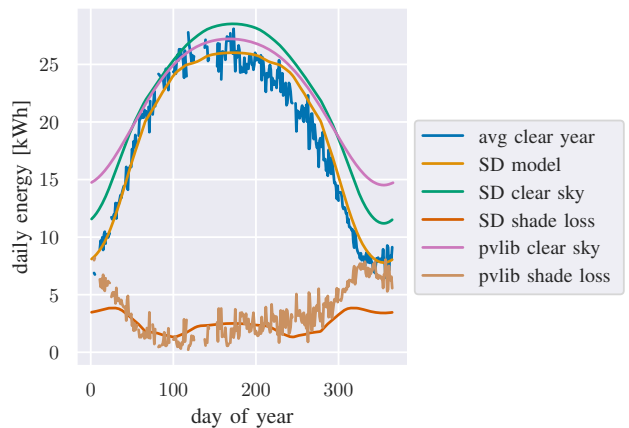


Fig. 6. Analysis of the shade OSD components that estimates the seasonal energy lost to shade.

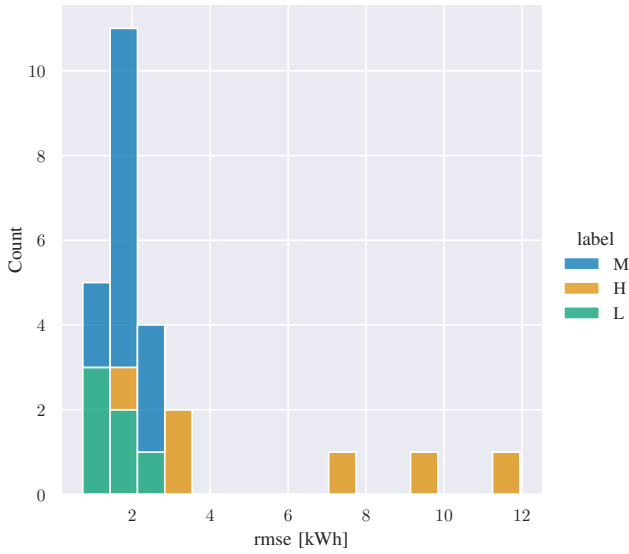


Fig. 7. Distribution of RMSE of seasonal shade loss across the fleet. The colors show the low, medium, and high shade bins.

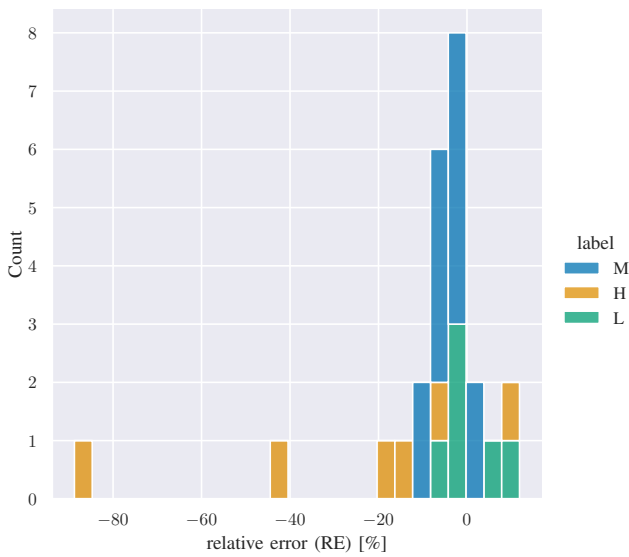


Fig. 8. Distribution of relative error (RE) across the fleet, which is defined as the difference between the SD model yearly loss estimate and the pvlib yearly loss estimate, normalized for total energy capture. The colors show the low, medium, and high shade bins.

model nonetheless estimates large yearly total shade losses for highly shaded sites, as shown in figure 10. As discussed with the case study, the SD model can be thought of as a lower bound on the shade losses.

C. Azimuth dependence

Having removed the large outliers in the “high shade” bin, we plot the RE versus the system azimuth angle in figure 11. We observe that there are positive relative errors for systems that have azimuths facing east (90°) and west

TABLE II
SUMMARY OF SD ERRORS

bin	RMSE		RE	
	mean	std	mean	std
L	1.63	0.60	0.65	6.26
M	1.83	0.52	-3.94	3.30
H	6.22	3.95	-26.1	35.3

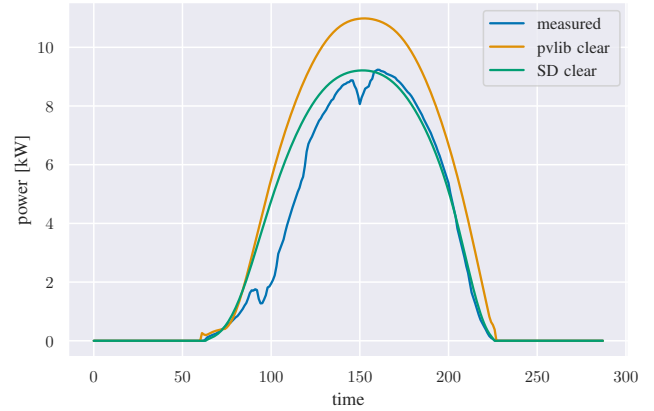


Fig. 9. A view of a single day of data (measured) and the pvlib and SD estimates of the clear sky envelope. This data was selected from the system in the high shade group with the worst error metrics. Note that the green line is below the orange line.

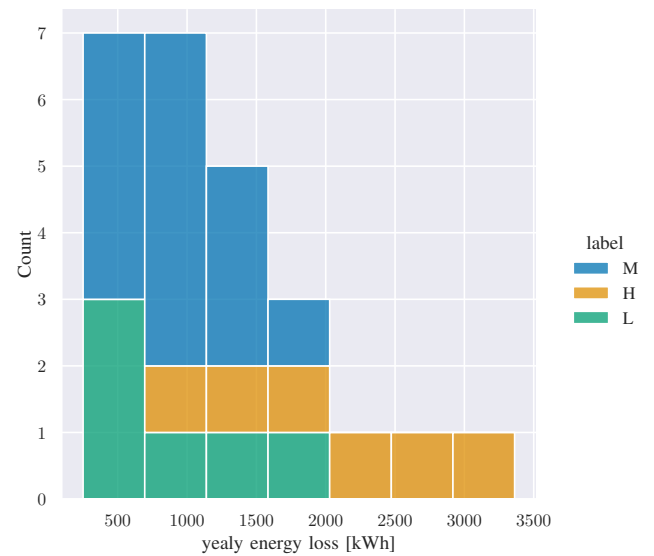


Fig. 10. Distribution of SD estimates total yearly energy lost to shading. As expected, the high shade sites have the largest total shade losses.

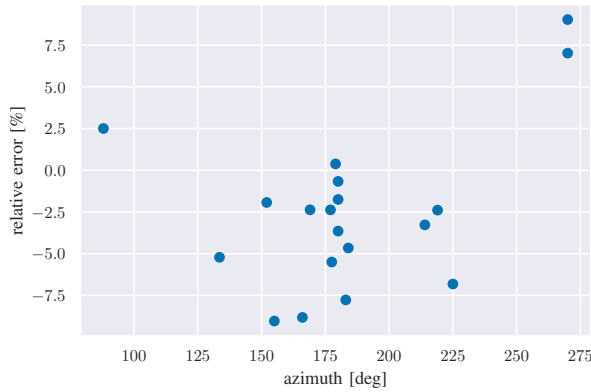


Fig. 11. The dependency of relative error on azimuth. The azimuth angle is defined with 0° being north and the angle increasing in the counterclockwise direction.

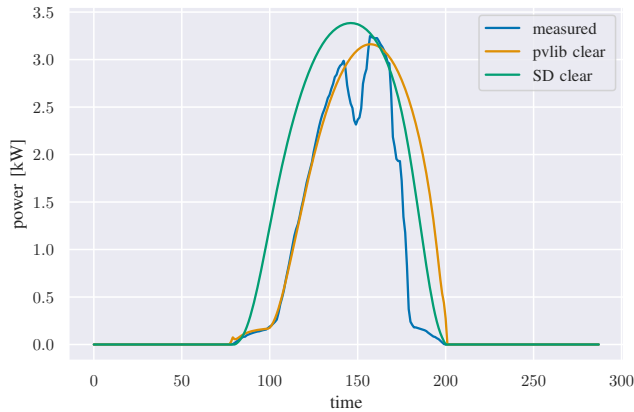


Fig. 12. A view of a single day from a system from the fleet that is oriented due west. Note that the green line is above the orange line.

(270°). We find that the SD model tends to over estimate the clear sky reference signal and therefore over estimate shade losses on system geometries that are due east or west. This behavior is clearly depicted in figure 12. In general, we find that the proposed methodology works quite well for systems that are oriented roughly between southwest and southeast directions. Improving the accuracy on systems that are outside that azimuth range will be an area of future research.

V. CONCLUSIONS

We present an application of a novel signal decomposition framework that is effective at analyzing shade losses in unlabeled PV data. This approach provides a tractable solution to estimating shade losses when no other information is available besides a power generation signal. While obviously hindered by not having access to e.g., reference systems or IV curves, our method is the first that is able to estimate shade loss to a reasonable degree of accuracy (usually within 10% to 15%) using just power data. This opens the door to the analysis of shade losses in fleets of distributed rooftop PV systems. We

expect to further improve the accuracy of these methods in future work, refining and developing the cost functions in the SD model to better account for all observed conditions and orientations.

ACKNOWLEDGMENTS

The authors would like to thank Prof. Stephen Boyd, Luke Volpatti, Gina Meyers-Im, and the GISMo Team at SLAC National Accelerator Laboratory their for input and feedback on this work. We also recognize the Seaborn plotting package for Python, which made the figures possible [23].

REFERENCES

- [1] M. Davis, C. Smith, B. White, R. Goldstein, X. Sun, M. Cox, G. Curtin, R. Manghani, S. Rumery, C. Silver, and J. Baca, *U.S. Solar market insight executive summary, 2020 year in review*. Wood Mackenzie and SEIA, 2021.
- [2] T. Townsend, C. Whitaker, B. Farmer, and H. Wenger, "New performance index for PV system analysis," *Conference Record of the IEEE Photovoltaic Specialists Conference*, vol. 1, pp. 1036–1039, 1994.
- [3] B. Meyers and S. Boyd, "Signal decomposition using masked proximal operators," pp. 1–60, feb 2022. [Online]. Available: <http://arxiv.org/abs/2202.09338>
- [4] B. Meyers, E. Apostolaki-Iosifidou, and L. Schelhas, "Solar data tools: Automatic solar data processing pipeline," in *2020 47th IEEE Photovoltaic Specialists Conference (PVSC)*, 2020, pp. 0655–0656.
- [5] B. Meyers, "solar-data-tools," may 2022. [Online]. Available: <http://dx.doi.org/10.5281/zenodo.6450368>
- [6] A. Woyte, J. Nijs, and R. Belmans, "Partial shadowing of photovoltaic arrays with different system configurations: literature review and field test results," *Solar Energy*, vol. 74, no. 3, pp. 217–233, mar 2003. [Online]. Available: <https://linkinghub.elsevier.com/retrieve/pii/S0038092X03001555>
- [7] C. Deline, "Partially shaded operation of a grid-tied PV system," in *2009 34th IEEE Photovoltaic Specialists Conference (PVSC)*. IEEE, jun 2009, pp. 001 268–001 273. [Online]. Available: <http://ieeexplore.ieee.org/document/5411246/>
- [8] B. Meyers and M. Mikofski, "Accurate modeling of partially shaded pv arrays," in *2017 IEEE 44th Photovoltaic Specialist Conference (PVSC)*. IEEE, jun 2017, pp. 3354–3359. [Online]. Available: <https://ieeexplore.ieee.org/abstract/document/8521559>
- [9] S. MacAlpine, C. Deline, and A. Dobos, "Measured and estimated performance of a fleet of shaded photovoltaic systems with string and module-level inverters," *Progress in Photovoltaics: Research and Applications*, vol. 25, no. 8, pp. 714–726, aug 2017. [Online]. Available: <http://dx.doi.org/10.1002/pip.1160https://onlinelibrary.wiley.com/doi/10.1002/pip.2884>
- [10] J. P. N. Torres, S. K. Nashih, C. A. Fernandes, and J. C. Leite, "The effect of shading on photovoltaic solar panels," *Energy Systems*, vol. 9, 2018.
- [11] A. Fairbrother, H. Quest, E. Özkalay, P. Wälchli, G. Friesen, C. Ballif, and A. Virtuani, "Long-term performance and shade detection in building integrated photovoltaic systems," *Solar RRL*, vol. 6, no. 5, p. 2100583, may 2022. [Online]. Available: <https://onlinelibrary.wiley.com/doi/10.1002/solr.202100583>
- [12] O. Tsafarakis, K. Sinapis, and W. G. J. H. M. van Sark, "A time-series data analysis methodology for effective monitoring of partially shaded photovoltaic systems," *Energies*, vol. 12, no. 9, p. 1722, may 2019. [Online]. Available: <https://www.mdpi.com/1996-1073/12/9/1722>
- [13] J. Liu, M. Wang, A. Curran, A. Maroof Karimi, W. Huang, E. Schnabel, M. Kohl, J. Braid, and R. French, "Real-world PV module degradation across climate zones determined from suns-v oc , loss factors and i-v steps analysis of eight years of i-v, p mp time-series datastreams," in *2019 IEEE 46th Photovoltaic Specialists Conference (PVSC)*. IEEE, jun 2019, pp. 0680–0686. [Online]. Available: <https://ieeexplore.ieee.org/document/8980541/>
- [14] T. Hastie, R. Tibshirani, and J. Friedman, *The Elements of Statistical Learning*, ser. Springer Series in Statistics. New York, NY: Springer New York, dec 2009. [Online]. Available: <http://ieeexplore.ieee.org/document/6727256/http://link.springer.com/10.1007/978-0-387-84858-7>

- [15] B. Meyers, "Estimation of soiling losses in unlabeled PV data," *Submitted to 2022 49th IEEE Photovoltaic Specialists Conference (PVSC)*, June 2022.
- [16] J. Duffie and W. Beckman, *Solar Engineering of Thermal Processes*, 4th ed. John Wiley, 2013.
- [17] S. Boyd and L. Vandenberghe, *Convex optimization*. Cambridge University Press, 2009.
- [18] W. F. Holmgren, C. W. Hansen, and M. A. Mikofski, "pvlib python: a python package for modeling solar energy systems," *Journal of Open Source Software*, vol. 3, no. 29, p. 884, sep 2018. [Online]. Available: <http://joss.theoj.org/papers/10.21105/joss.00884>
- [19] G. Golub and C. Van Loan, *Matrix Computations*, 3rd ed. Baltimore, MD: Johns Hopkins University Press, 1996.
- [20] S. Boyd and L. Vandenberghe, *Introduction to Applied Linear Algebra*, 2018.
- [21] D. F. Florez Rodriguez and B. Meyers, "Solar panel power simulation for shade detection," *Submitted to 2022 49th IEEE Photovoltaic Specialists Conference (PVSC)*, June 2022.
- [22] P. Ineichen, "A broadband simplified version of the solis clear sky model," *Solar Energy*, vol. 82, no. 8, pp. 758–762, 2008. [Online]. Available: <https://www.sciencedirect.com/science/article/pii/S0038092X08000406>
- [23] M. L. Waskom, "seaborn: statistical data visualization," *Journal of Open Source Software*, vol. 6, no. 60, p. 3021, 2021. [Online]. Available: <https://doi.org/10.21105/joss.03021>